

# Delocalized electronic states in small clusters. Comparison of $\text{Na}_n$ , $\text{Cu}_n$ , $\text{Ag}_n$ , and $\text{Au}_n$ clusters

H. Handschuh <sup>a</sup>, Chia-Yen Cha <sup>a</sup>, H. Möller <sup>b</sup>, P.S. Bechthold <sup>a</sup>,  
G. Ganteför <sup>a</sup>, W. Eberhardt <sup>a</sup>

<sup>a</sup> *Institut für Festkörperforschung, Forschungszentrum Jülich, D-52425 Jülich, Germany*

<sup>b</sup> *Fakultät für Physik, Universität Bielefeld, D-33615 Bielefeld, Germany*

## Abstract

Photoelectron spectra of  $\text{Na}_n^-$ ,  $\text{Cu}_n^-$ ,  $\text{Ag}_n^-$ , and  $\text{Au}_n^-$  clusters reveal the electronic structure of these particles. The experimental results are compared to the predictions of quantum chemical calculations and of the shell model. The spectra of  $\text{Ag}_n^-$  allow for a stringent test of both approaches, because most of the observed features are assigned to s-derived orbitals and they also display much sharper features than the alkali data. A qualitative equivalence of the electronic shell model with high-level quantum chemical calculations in terms of the symmetries of the involved single particle orbitals is found for the delocalized states derived from the atomic s-electrons.

## 1. Introduction

Photoelectron spectroscopy has proven to be the proper tool to reveal the electronic structure of atoms and molecules. The problem of mass separation preventing the application of this technique to neutral clusters has been solved by the development of the photoelectron spectroscopy of negatively charged clusters (anions) [1–5]. We applied this technique to the study of clusters of anions of simple metals with  $n=2$ –20 atoms, and have obtained spectra of  $\text{Na}_n^-$ ,  $\text{Cu}_n^-$ ,  $\text{Ag}_n^-$ , and  $\text{Au}_n^-$  clusters with an energy resolution sufficient to reveal details of the electronic structure.

The theoretical description of the electronic structure of these clusters is based upon two seemingly different models. Several experimentally determined properties of clusters of simple metals such as the alkali metals and the coinage metals (Cu, Ag, Au) can be qualitatively described by the electronic shell

model [6]. The electrons are assumed to be delocalized completely within the cluster boundaries. Accordingly the electrons occupy electronic shells with a well-defined angular momentum. In this model the addition of one atom to the cluster corresponds to the addition of one more electron into the total potential well. The simultaneous change in the geometry of the cluster may result in a change of the degeneracy of the shells.

In contrast to this description the small clusters can be considered as individual molecules with varying symmetries [7–9]. The molecular orbitals are different for each cluster and a common pattern or a systematic development of the electronic structure with cluster size is not predictable.

Recently, quantum chemical ab initio calculations of the electronic structure of metal cluster anions up to  $n \sim 10$ , including a detailed analysis of the calculated electronic states have become available [7,10]. In the present Letter, we will compare these exact cal-

culations with our data. Furthermore, the exact assignments will be compared to assignments based on the shell model [6].

## 2. Experimental

The experimental apparatus is described in detail elsewhere [5]. The anions are generated either by a laser vaporization source (Ag, Au) or by a pulsed arc cluster ion source (PACIS) (Na, Cu). The PACIS design used for the generation of alkali clusters is similar to the one used for Ga, but all parts close to the discharge have been manufactured from molybdenum. The insulators are made of quartz-glass. The negatively charged clusters are directly generated in the source and cooled in a supersonic expansion. The vibrational temperature of  $\text{Au}_2^-$  has been determined from a high resolution spectrum to be  $200 \pm 70$  K [11,12]. The temperature of the  $\text{Na}_n^-$  clusters could not be directly determined, but the features in the spectra exhibit similar or smaller linewidths than in earlier experiments [3] using a continuous oven source.

The anions are accelerated by a pulsed electric field resulting in a mass separation due to their time-of-flight. While passing the center of an electron spectrometer a selected bunch of anions is decelerated by a pulsed electric field and irradiated by a UV-laser pulse. The UV-laser pulse is generated using an excimer laser (ArF,  $h\nu = 6.42$  eV,  $1$  mJ/cm<sup>2</sup>; KrF,  $h\nu = 5.0$  eV,  $10$  mJ/cm<sup>2</sup>) or a Nd:YAG laser (3rd harmonic,  $h\nu = 3.49$  eV,  $0.1$  J/cm<sup>2</sup>; 4th harmonic,  $h\nu = 4.66$  eV,  $0.1$  J/cm<sup>2</sup>). The kinetic energy of the detached electrons is measured by a 'magnetic bottle'-type electron time-of-flight spectrometer [5]. The energy resolution depends on the kinetic energy of the electrons and the velocity of the clusters (Doppler effect) and varies between  $0.1$  eV and  $5$  meV [12].

## 3. Results and discussion

The electronic shell model can only be applied to clusters of metals with highly delocalized valence electrons [6]. This corresponds to a description of the bandstructure of the bulk metal by a dispersion

curve  $E(k)$  similar to a free electron parabola. This is approximately valid for the alkali metals and the s-derived density of states [13] of the coinage metals (Cu, Ag, Au). In all cases these s-derived states exhibit a strong s-p hybridization, which, however, does not significantly alter the degree of delocalization. The valence band of e.g. Na is mainly s-derived with a bandwidth of  $3.5$  eV and a work function of  $2.3$  eV. The s-derived states of Cu and Ag have a bandwidth of about  $9.5$  and  $7.4$  eV and a work function of  $4.3$  and  $4.6$  eV, respectively. For Cu, the total density of states is dominated by s-states up to  $1.9$  eV below the Fermi energy. For Ag, the d-derived states are located at about  $2$  eV higher BE with respect to Cu. Au is basically similar to Cu with a slightly higher work function of  $4.8$  eV and a larger influence of relativistic effects and a strong spin-orbit interaction.

Fig. 1 displays a comparison of  $\text{Na}_n^-$  and  $\text{Ag}_n^-$  clusters with  $n=2, 3, 4$ . Each feature corresponds to a transition from the electronic ground state of the anion into the ground and excited states of the neutral. For  $\text{Ag}_n^-$  only excited states involving s-electrons are observed in Fig. 1, since excited states involving d-electrons are expected at excitation energies beyond  $4$  eV with respect to the neutral ground state [7]. The symmetries of the neutral final states deduced from HF-CI calculations [7,10] are indicated in the figure. The spectra of the dimers and trimers are basically similar as expected from the above considerations. The binding energies differ by a scaling factor of about 2 corresponding to the differences in valence bandwidths of the two bulk metals.

The spectra of the two tetramers are different, since their geometries are different.  $\text{Na}_4^-$  is predicted to be linear [10], while  $\text{Ag}_4^-$  is probably a planar rhombus [7]. Apart from these geometry-induced differences, the electronic structure of Ag and Na clusters is similar. In general, the features observed in the  $\text{Na}_n^-$  spectra [3] are much broader than for  $\text{Ag}_n^-$ . This has also been observed for larger clusters [3] of  $\text{K}_n^-$ . The reason might be the fluxional character of these relatively weakly bound alkali clusters. Because much more detail can be observed in the  $\text{Ag}_n^-$  spectra, we consider Ag as a model material for the study of the s-derived density of states in simple metals, with the restriction that the discussion is limited to excited

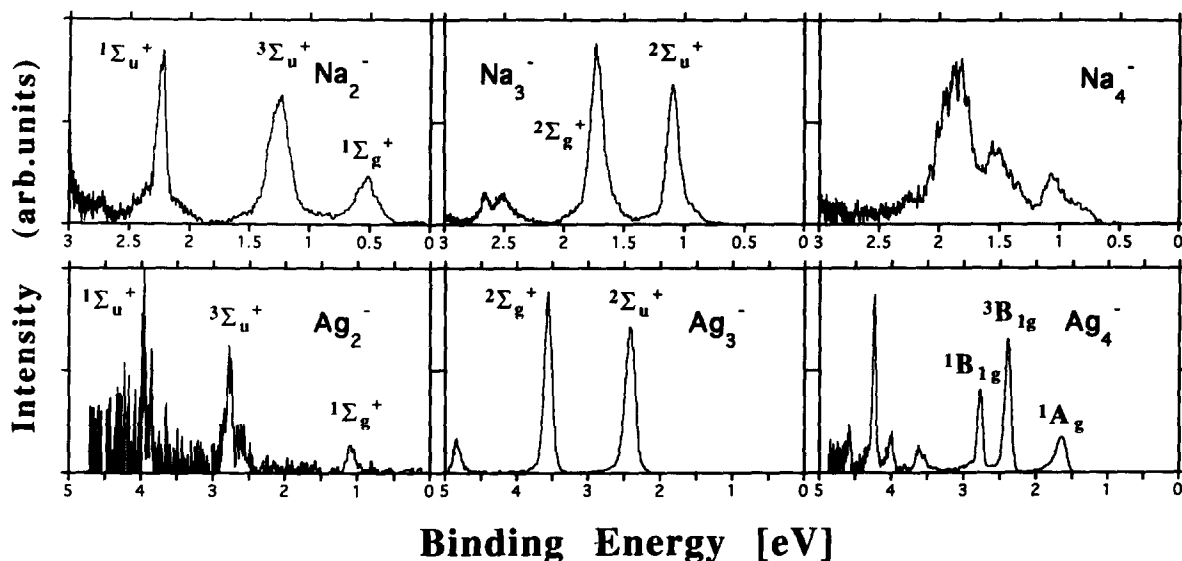


Fig. 1. Comparison of photoelectron spectra of  $\text{Ag}_n^-$  and  $\text{Na}_n^-$  clusters with  $n=2, 3, 4$ . The spectrum of  $\text{Ag}_3^-$  is recorded with  $h\nu=6.42$  eV,  $\text{Ag}_2^-$  and  $\text{Ag}_4^-$  with  $h\nu=5.0$  eV and the spectra of the  $\text{Na}_n^-$  clusters with  $h\nu=3.55$  eV photon energy. The spectra of the dimers and trimers exhibit a certain similarity, while the tetramer data are different. For a few selected features the assignments [2,13,16] of the neutral final states are indicated.

states which are not more than about 4 eV above the neutral ground state.

Fig. 2 displays a comparison of the spectra of  $\text{Ag}_4^-$  and  $\text{Ag}_3^-$  with the corresponding data of Cu [14] and Au [15]. The spectra of  $\text{Cu}_4^-$  and  $\text{Cu}_3^-$  are similar to the Ag data within a range of 2 eV above the neutral ground state, which is in agreement with the expectations derived from the discussion of the bulk electronic structure above. Beyond about 4.5 eV BE the Cu spectra are dominated by d-derived states.  $\text{Au}_4^-$  and  $\text{Au}_3^-$  display a limited similarity to the corresponding data of Cu and Ag. In general, the spectra of the Au clusters [15] display many more features and fine structures than those of Cu and Ag. An assignment of these features is not possible at present. A reason for the complexity of the Au data is probably the strong spin-orbit interaction in these heavy atom clusters. The s-derived features also exhibit a spin-orbit splitting, because these states have a strong 6p admixture (s-p hybridization) [1,15].

HF-CI calculations [7] of the transitions observed in  $\text{Ag}_n^-$  photoelectron spectra are available up to  $n=9$ . A detailed comparison will be given elsewhere [16]. In the present Letter, we will demonstrate the state of the analysis taking  $\text{Ag}_4^-$  as an example. According to

the calculations and our high-resolution vibrational data [12]  $\text{Ag}_4^-$  is a planar rhombus. The electronic ground state of the anion is  ${}^2\text{B}_{2u}$ . The features observed in the spectrum displayed in Fig. 1 are assigned to transitions into the ground and excited electronic states of the neutral clusters ( ${}^1\text{A}_g$ ,  ${}^3\text{B}_{1g}$ ,  ${}^1\text{B}_{1g}$ , ...). In general, the assignments to the calculated transitions cannot be based on the BEs alone, because the calculated values differ in some cases by 0.1–0.3 eV from the experimentally determined ones. The assignments are supported, however, by the comparison [16] of spectra recorded at different photon energies and the comparison with the corresponding Cu data.

The calculated transition energies [7] and the experimental data [16] for  $n=2-9$  are summarized in Fig. 3. The available pairs of measured and calculated BEs of the ground state transition (=vertical detachment energy) and the transitions into the first, second, third and fourth, excited states of the neutral cluster are displayed. The agreement between experiment and theory is almost perfect for  $n=2-6$ , whereas the patterns for  $\text{Ag}_{7-9}$  are slightly different. Despite the slight discrepancies the agreement between experiment and theory is reasonably good and,

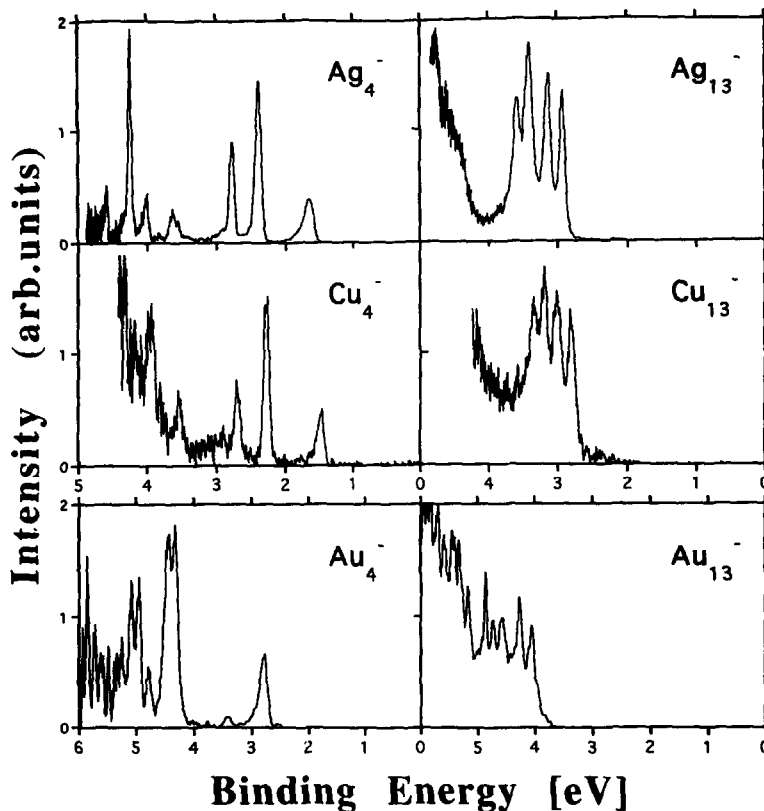


Fig. 2. Photoelectron spectra of the 4-atom and 13-atom cluster anions of Ag, Cu and Au. The spectra of Ag and Cu are recorded with a photon energy of  $h\nu=5.0$  eV, the spectra of the Au clusters with  $h\nu=6.4$  eV. The binding energy ranges from 0–5 eV for Cu and Ag and from 0–6 eV for Au.

therefore, the electronic structure of these clusters (except  $\text{Ag}_7^-$ ) can be considered to be well described by the quantum chemical calculation.

However, the pattern of various electronic states displayed in Fig. 3 does not reveal trends and similarities, which might be helpful in the understanding of the development of the electronic structure with increasing cluster size. In the following, we will try to identify similarities of the electronic structures of the  $\text{Ag}_n^-$  clusters. For this purpose it is necessary, to represent each electronic state by a simplified and therefore less accurate pattern. The simplification will take place in two steps and will be illustrated for  $\text{Ag}_4^-$ .

The first step is the assignment of the features in the spectra to photoemission from occupied single particle orbitals in the anion. This is possible, if the involved electronic states can be represented by a configuration of single particle orbitals. E.g., the

ground state  ${}^2\text{B}_{2u}$  of the  $\text{Ag}_4^-$  has the configuration  $a_2^2 b_{3u}^2 b_{2u}^1$ . The first excited state  ${}^3\text{B}_{1g}$  of neutral  $\text{Ag}_4$  has the configuration  $a_2^2 b_{3u}^1 b_{2u}^1$ . Since the two configurations differ by the lack of one electron in the  $b_{3u}$  orbital only, the corresponding peak is assigned to direct photoemission from this orbital. However, these straight forward assignments are hampered by three effects, which have to be taken into consideration:

(1) *Multiplet splitting*. The second excited state  ${}^1\text{B}_{1g}$  of  $\text{Ag}_4$  has the same electronic occupation as the  ${}^3\text{B}_{1g}$  state [7]. The configuration has two unpaired electrons, which can combine to a singlet or a triplet state with a slightly different energy. Therefore, the photoemission from the  $b_{3u}$  orbital of  $\text{Ag}_4^-$  yields a doublet with a characteristic energy spacing and intensity ratio. The BE of such an orbital is usually taken as the 'center of gravity' of the two features [17].

(2) *Shake-up processes*. There are various transi-

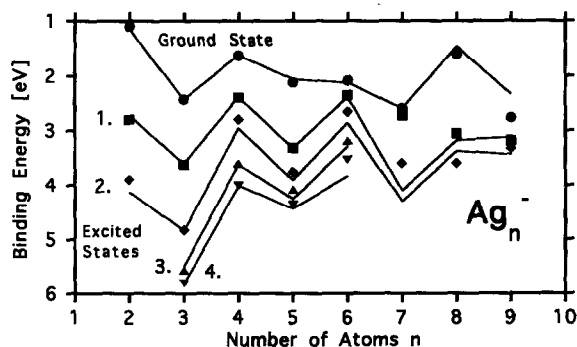


Fig. 3. Comparison of the calculated [7] and experimentally determined energies [16] of the transitions observed in photoelectron spectra of  $\text{Ag}_n^-$  clusters with  $n=2-9$ . The features correspond to transitions from the electronic ground state of the anion into the neutral and excited electronic states of the neutral cluster. The calculated values are connected by lines as a guide for the eye. The experimental values are marked by various symbols for the different final states ((●) ground state; (■) first excited state; (◆) second excited state; (▲) third excited state; (▼) fourth excited state).

tions into states, whose configurations differ from the ground state configuration of the anion by more than one electron. E.g., a possible configuration is  $a_g^2 b_{2u}^2$ . A transition into this configuration involves two electrons: the photoemission of one of the electrons from the  $b_{3u}$  orbital and the excitation of the other one into the  $b_{2u}$  orbital.

(3) *Configuration mixing*. Higher excited states of a particle might not be represented by a single configuration, but be a linear combination of various configurations such as

$${}^x Y_Z = A(\text{conf. 1}) + B(\text{conf. 2}) + C(\text{conf. 3}) + \dots$$

As long as the factor  $A$  is close to 1 the state  ${}^x Y_Z$  is more or less correctly described by configuration 1. However, if this factor is smaller than 0.7 the contribution from this configuration is smaller than 50% and therefore the assignment of  ${}^x Y_Z$  to a single configuration is inappropriate.

Despite these difficulties the features in the spectra can be tentatively assigned to emission from various single particle orbitals in the clusters [16]. The second step of simplification is the comparison of these orbitals for different clusters. For this purpose, details of the geometry have to be neglected and the basic symmetry properties have to be extracted. Within the framework of the shell model [6] these single

particle orbitals can be classified into s-, p-, d- and f-like orbitals.

This is illustrated in Fig. 4 for  $\text{Ag}_4$  assuming  $D_{2h}$  symmetry. The  $a_g$  orbital has the same symmetry as a 1s orbital. In a simple LCAO picture it can be considered as a constructive superposition of all four atomic s-orbitals. The resulting molecular orbital has an obvious, albeit limited, similarity to a spherical s-orbital. This comparison gives a measure of the degree of uncertainty introduced by such an assignment. With increasing cluster size and increasing number of atomic orbitals ordered in a more or less spherical arrangement the overlap between this lowest LCAO orbital and the s-orbital increases. Similar considerations can be made for the higher single particle orbitals (see Fig. 4). The overlap between such shell model orbitals with s, p and d character and calculated molecular orbitals has been calculated for neutral  $\text{Na}_n$  clusters by Röhrlisberger and Andreoni [8]. They found overlaps varying between (50%) and (70%) for clusters with 5–20 atoms.

Fig. 5 displays the results of the assignments of the  $\text{Ag}_n^-$  data up to  $n=21$  [16]: the electronic shell structure of the s-derived density of states of  $\text{Ag}_n^-$  clusters.

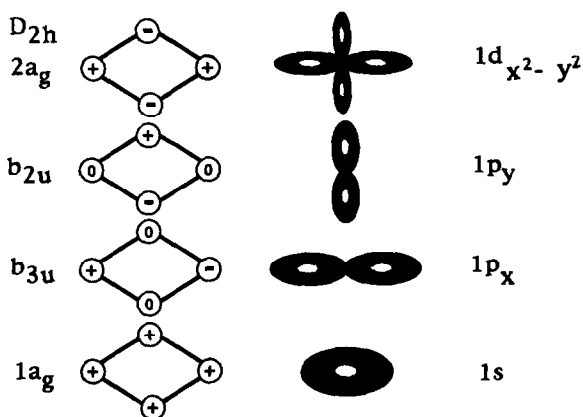


Fig. 4. Illustration of the equivalence of the symmetries of the single particle orbitals calculated in the HF-CI scheme [7] (first column:  $1a_g, b_{3u}, b_{2u}, 2a_g$ ) with the shell model orbitals (fourth column:  $1s, 1p_x, 1p_y, 1d_{x^2-y^2}$ ) for  $\text{Ag}_4^-$ . In a simple LCAO picture (excluding atomic p-orbitals), the HF orbitals can correspond to linear combinations of atomic s-orbitals with the coefficients +1, 0 or -1. The coordinates of these orbitals and the coefficients are sketched in the second column. In the third column the shape of the shell model orbitals is sketched. The  $1a_g, b_{3u}$  and  $b_{2u}$  orbitals are occupied in  $\text{Ag}_4^-$ .

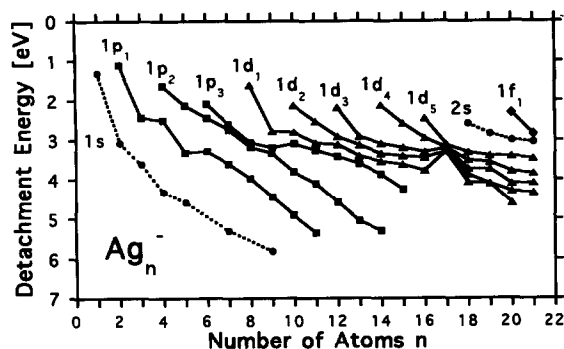


Fig. 5. The detachment energies (DEs) of the single particle orbitals extracted from the spectra for the  $\text{Ag}_n^-$  cluster. If multiplets are observed, the 'center of gravity' of the two peaks is taken as the DE. The orbitals are assigned with increasing BE to the  $1s$ ,  $1p_1$ ,  $1p_2$ ,  $1p_3$ ,  $1d_1$ ,  $1d_2$ ,  $1d_3$ ,  $1d_4$ ,  $1d_5$ ,  $2s$ ,  $1f_1$  subshells. For the clusters, where calculations are available, the symmetries of the shell model orbitals correspond to the symmetries of the exact single particle orbitals.

The detachment energies (DE) of the orbitals given in the figure correspond to the position of the features in the spectra. These DEs do not correspond to the BEs of the calculated shells because of the relaxation. Therefore, the DEs are significantly smaller than the BEs.

Fig. 5 can be discussed in terms of the ellipsoidal shell model [6].  $\text{Ag}_7^-$  is not spherical, but has an oblate shape with two p levels at low DE and one at high DE. A pronounced shell closing is observed at  $n=17$ . The five 1d levels are almost degenerate. We believe this cluster is the smallest one with an almost spherical geometry. At  $n=19$ , a second shell closing corresponding to 20 electrons is expected [6]. However, no degeneracy of the 1d levels indicating a higher symmetry is observed. A possible explanation might be the tendency of a 19-atom cluster to assume a capped icosahedral shape corresponding to a prolate deformation.

#### 4. Conclusion

A comparison of photoelectron spectra of  $\text{Na}_n^-$ ,  $\text{Cu}_n^-$ ,  $\text{Ag}_n^-$ , and  $\text{Au}_n^-$  clusters demonstrates the similarity of the low lying excited electronic states of  $\text{Na}_n^-$  and  $\text{Ag}_n^-$  clusters. Photoelectron spectra of  $\text{Ag}_n^-$  clusters with  $n=2-9$  have been compared to HF-CI calculations [7] resulting in an exact assignment

of almost all observed features to transitions from the anion ground state to various neutral electronic states.

Based on the calculations, in a first step of simplification the data are reassigned using the single particle approximation. Multiplet splitting, shake-up processes and configuration mixing are qualitatively considered. In a second step the single particle orbitals are compared to angular momentum eigenstates (= electronic shells). It is found, that the exact HF orbitals have the same symmetry as the shell model orbitals.

We found both theoretical approaches, the shell model [6] and the quantum chemical HF-CI scheme [7], to be equivalent in terms of the involved symmetries of the single particle orbitals. The quantum chemical calculations correspond to an exact quantitative description of the photoelectron spectra, while the shell model consideration yields a qualitative understanding of the development of the electronic structure with increasing cluster size. The two models do not necessarily contradict each other.

#### Acknowledgement

We thank V. Bonačić-Koutecký for lively and encouraging discussions and the sharing of new unpublished results of calculations and H. Pfeifer and J. Lauer for their technical support.

#### References

- [1] J. Hoe, K.M. Ervin and W.C. Lineberger, *J. Chem. Phys.* 93 (1990) 6987.
- [2] K.J. Taylor, C.L. Pettiette-Hall, O. Cheshnovsky and R.E. Smalley, *J. Chem. Phys.* 96 (1992) 3319.
- [3] K.M. McHugh, J.G. Eaton, G.H. Lee, H.W. Sarkas, L.H. Kidder, J.T. Snodgrass, M.R. Manaa and K.H. Bowen, *J. Chem. Phys.* 91 (1989) 3792.
- [4] G. Ganteför, M. Gausa, K.H. Meiwes-Broer and H.O. Lutz, *Faraday Discussions Chem. Soc.* 86 (1988) 1.
- [5] C.-Y. Cha, G. Ganteför and W. Eberhardt, *Rev. Sci. Instr.* 63 (1992) 5661.
- [6] W. de Heer, *Rev. Mod. Phys.* 65 (1993) 611.
- [7] V. Bonačić-Koutecký, L. Cespiva, P. Fantucci, J. Pittner and J. Koutecký, *J. Chem. Phys.* 100 (1994) 490, and references therein; V. Bonačić-Koutecký, private communication.
- [8] U. Röthlisberger and W. Andreoni, *J. Chem. Phys.* 94 (1991) 8129.
- [9] R.O. Jones, *Phys. Rev. Letters* 67 (1991) 224.

- [10] V. Bonačić-Koutecký, P. Fantucci and J. Koutecký, *J. Chem. Phys.* 91 (1989) 3794.
- [11] G.F. Gantefor, D.M. Cox and A. Kaldor, *J. Chem. Phys.* 93 (1990) 8395.
- [12] H. Handschuh, P.S. Bechthold, G. Ganteför and W. Eberhardt, to be published.
- [13] V.L. Moruzzi, J.F. Janak, A.R. Williams, *Calculated electronic properties of metals* (Pergamon Press, Oxford, 1981).
- [14] C.-Y. Cha, G. Ganteför and W. Eberhardt, *J. Chem. Phys.* 99 (1993) 6308.
- [15] H. Handschuh, G. Ganteför, P.S. Bechthold and W. Eberhardt, *J. Chem. Phys.* 100 (1994) 7093, and references therein; unpublished data.
- [16] H. Handschuh, C.-Y. Cha, P.S. Bechthold, G. Ganteför and W. Eberhardt, to be published.
- [17] J. Berkowitz, *Photoabsorption, photoionisation and photoelectron spectroscopy* (Academic Press, New York, 1979).